^{16}O Electroweak Response Functions from First Principles

Bijaya Acharya,[1,*] Joanna E. Sobczyk,[2,†] Sonia Bacca,[2,3,‡] Gaute Hagen,[1,4,§] and Weiguang Jiang[5,‖]
[1]Physics Division, Oak Ridge National Laboratory, Oak Ridge, Tennessee 37831, USA
[2]Institut für Kernphysik and PRISMA$^+$ Cluster of Excellence, Johannes Gutenberg-Universität, 55128 Mainz, Germany
[3]Helmholtz-Institut Mainz, Johannes Gutenberg-Universität Mainz, D-55099 Mainz, Germany
[4]Department of Physics and Astronomy, University of Tennessee, Knoxville, Tennessee 37996, USA
[5]Mainz Institut für Theoretical Physics and PRISMA$^+$ Cluster of Excellence, Johannes Gutenberg-Universität, 55128 Mainz, Germany

(Received 10 October 2024; accepted 2 May 2025; published 19 May 2025)

We present calculations of various electroweak response functions for the ^{16}O nucleus obtained using coupled-cluster theory in conjunction with the Lorentz integral transform method. We employ nuclear forces derived at next-to-leading order and next-to-next-to-leading order in chiral effective field theory and perform a Bayesian analysis to assess uncertainties. Our results are in good agreement with available electron-scattering data at $|\mathbf{q}| \approx 326$ MeV/c. Additionally, we provide several predictions for the weak response functions in the quasielastic peak region at $|\mathbf{q}| = 300$ and 400 MeV/c, which are critical for long-baseline neutrino experiments.

DOI: 10.1103/PhysRevLett.134.202501

Introduction—While the standard model accurately describes the interactions of leptons with elementary particles, the cross sections for leptons interacting with atomic nuclei involve significantly larger theoretical uncertainties. This is due to the fact that the nucleus is a complex many-body system composed of protons and neutrons held together by the strong force in a nonperturbative regime [1–3]. Recent advancements in nuclear theory have made substantial progress in calculating nuclear properties, including both static and, to a lesser extent, dynamic properties [4,5]. The use of chiral effective field theory [6–8] in combination with modern computational tools, often referred to as the *ab initio* approach [9,10], holds the greatest promise for quantifying and potentially reducing uncertainties.

In addition to providing a powerful means of probing nuclear structure, lepton-nucleus scattering is crucial for both astrophysics and particle physics. In astrophysics, the detection of neutrinos with energies on the order of 10 MeV originating from a supernova explosion in our Galaxy can provide insights into the progenitor and the explosion mechanism [11]. In particle physics, the discovery that neutrinos have nonzero masses and undergo oscillations is among the most groundbreaking findings of this century. Understanding the oscillation mechanism through long-baseline neutrino experiments will be a major focus of physics research in the coming decades [12,13]. Unlike the (e, e') case, where the initial and final electron energies are known, the incident neutrino energies must be reconstructed in these experiments. Accurate interpretation of the data on neutrino masses and mixing angles depends on reliable calculations of neutrino-nucleus scattering, particularly in the quasielastic kinematic regime at energies from a few hundred MeV to a few GeV [14]. Interestingly, in this range, precise electron-scattering experiments can be used to cross-check the implementation of the weak current operators, whose vector parts are the electromagnetic current operators that are probed by electron-scattering experiments. Furthermore, comparison with existing electron-scattering data also provides a validation of the treatment of the many-body dynamics.

Numerous (e, e') cross section measurements have been conducted in the past for stable nuclei across the nuclear chart [15]. Among the nuclear targets relevant for the long-baseline neutrino program, the most extensively studied nucleus is ^{12}C, while ^{16}O and ^{40}Ar remain comparatively less explored [16–27]. In the standard shell-model picture, both ^{12}C and ^{16}O are closed-shell nuclei, whereas ^{40}Ar is an open-shell nucleus. ^{12}C has been extensively investigated using Quantum Monte Carlo methods [28–30]. The α-cluster structure of its ground and excited states [31,32] presents challenges for several other *ab initio* approaches. In contrast, inelastic scattering observables for the heavier nuclei ^{16}O and ^{40}Ar remain unexplored within an *ab initio* framework, although elastic scattering off ^{40}Ar has been studied [33].

*Contact author: acharyabn@ornl.gov
†Contact author: jsobczyk@uni-mainz.de
‡Contact author: s.bacca@uni-mainz.de
§Contact author: hageng@ornl.gov
‖Contact author: wjiang@uni-mainz.de

Published by the American Physical Society under the terms of the Creative Commons Attribution 4.0 International license. Further distribution of this work must maintain attribution to the author(s) and the published article's title, journal citation, and DOI.

In this Letter, we focus on the inelastic lepton-scattering observables of ^{16}O for the first time within the *ab initio* approach. Our method of choice is the coupled-cluster theory [34–38], a well-established many-body method which scales polynomially with the system size. We use nuclear forces derived from chiral effective field theory [6–8]. Our approach links directly to the fundamental interactions of the standard model up to rigorous uncertainty estimates. This is an essential step toward a similar treatment of ^{40}Ar, enabled by recent advances in *ab initio* methods for open-shell nuclei [39–42].

Theory—The inclusive differential cross sections for the electron-scattering $^{16}\mathrm{O}(e,e')$ reaction and the charged-current neutrino(antineutrino) scattering $^{16}\mathrm{O}(\nu_e,e)/^{16}\mathrm{O}(\bar{\nu}_e,e^+)$ reactions can be written as [5,43]

$$\begin{aligned}\frac{d^2\sigma_e}{d\Omega d\epsilon'} &= \sigma_M\left[\frac{Q^4}{q^4}R_L(\omega,q)+\left(\tan^2\frac{\theta}{2}+\frac{Q^2}{2q^2}\right)R_T(\omega,q)\right]\\ \frac{d^2\sigma_{\nu/\bar{\nu}}}{d\Omega d\epsilon'} &= \frac{G_F^2}{2\pi^2}k'E'\cos^2\frac{\theta}{2}\left[R_{00}(\omega,q)+\frac{\omega^2}{q^2}R_{zz}(\omega,q)\right.\\ &\quad -\frac{\omega}{q}R_{0z}(\omega,q)+\left(\tan^2\frac{\theta}{2}+\frac{Q^2}{2q^2}\right)R_{xx}(\omega,q)\\ &\quad \left.\mp\tan\frac{\theta}{2}\sqrt{\tan^2\frac{\theta}{2}+\frac{Q^2}{q^2}}R_{xy}(q,\omega)\right].\end{aligned} \tag{1}$$

Here, σ_M is the Mott cross section, G_F is the Fermi constant, E' and k' are the energy and momentum of the outgoing lepton, $+/-$ correspond to the neutrino and antineutrino, respectively, and $R_{\mu\nu}$ are the dynamical response functions that depend on the energy transfer ω and the momentum transfer $\mathbf{q}$, with $Q^2=q^2-\omega^2$. We take the momentum transfer $q=|\mathbf{q}|$ along the z axis, such that x and y are the transverse components of the current operator. The response functions are, in general, given by

$$R_{\alpha\beta}(\omega,q)=\sum_f\langle\Psi_f|j_\alpha|\Psi_0\rangle\langle\Psi_f|j_\beta|\Psi_0\rangle^*\delta(\omega+E_0-E_f), \tag{2}$$

where $|\Psi_0\rangle$ and $|\Psi_f\rangle$ are the nuclear ground and excited states with energy E_0 and E_f, respectively, and j_α is the four-vector current operator. For electron scattering, we separate the current in isoscalar (S) and isovector (V) parts as $j_\alpha=j_\alpha^{(S)}+j_\alpha^{(V)}$, and we denote the only two nonvanishing response functions R_{00} and R_{xx} as R_L and R_T, respectively. The timelike and spacelike components of the isoscalar electromagnetic four-vector current $j_\alpha^{(S)}$ are given by

$$j_0^{(S)}=G_E^S(Q^2)e^{i\mathbf{q}\cdot\mathbf{r}_j}\frac{1}{2}, \tag{3}$$

and

$$\mathbf{j}^{(S)}=\left(G_E^S(Q^2)\frac{\bar{\mathbf{p}}_j}{m}-iG_M^S(Q^2)\frac{\mathbf{q}\times\boldsymbol{\sigma}_j}{2m}\right)e^{i\mathbf{q}\cdot\mathbf{r}_j}\frac{1}{2}, \tag{4}$$

respectively. Here, $G_{E,M}^S\equiv G_{E,M}^p+G_{E,M}^n$ are the isoscalar electric and magnetic form factors, and $\bar{\mathbf{p}}_j=(\mathbf{p}_j'+\mathbf{p}_j)/2=\mathbf{p}_j+\mathbf{q}/2$ is the average of the initial and final momenta of the nucleon. In chiral effective field theory, Eq. (3) contributes at leading order and Eq. (4) is suppressed by one power of the expansion parameter p/Λ_χ, where p is the typical momentum of the process and Λ_χ is the breakdown scale of the theory. The expressions for the isovector electromagnetic current operator, $j_\alpha^{(V)}$, can be obtained from the substitutions $1/2\to\tau_{j,z}/2$ and $G_{E,M}^S\to G_{E,M}^V\equiv G_{E,M}^p-G_{E,M}^n$.

For neutrino scattering, the charge-changing weak current is taken as the sum of the vector term $j_\alpha^{(\pm)}$, which is related to $j_\alpha^{(V)}$ by a rotation in isospin space, $\tau_{j,z}/2\to\tau_{j,\pm}\equiv(\tau_{j,x}\pm i\tau_{j,y})/2$, and the axial term $j_\alpha^{5(\pm)}$. Here, the spacelike component

$$\mathbf{j}_\alpha^{5(\pm)}=-G_A(Q^2)\left(\boldsymbol{\sigma}_j-\frac{\mathbf{q}\boldsymbol{\sigma}_j\cdot\mathbf{q}}{m_\pi^2+q^2}\right)e^{i\mathbf{q}\cdot\mathbf{r}_j}\frac{\tau_{j,\pm}}{2} \tag{5}$$

appears at the same order as Eq. (3), and the timelike (axial charge) component

$$j_0^5=-G_A(Q^2)\left(\boldsymbol{\sigma}_j\cdot\frac{\bar{\mathbf{p}}_j}{m}-\frac{\omega\boldsymbol{\sigma}_j\cdot\mathbf{q}}{m_\pi^2+q^2}\right)e^{i\mathbf{q}\cdot\mathbf{r}_j}\frac{\tau_{j,\pm}}{2} \tag{6}$$

is suppressed by a factor of p/Λ_χ, i.e., it contributes at the same order as Eq. (4). In Eqs. (5) and (6), the pion-pole diagrams have been expressed in terms of the axial form factor $G_A(Q^2)$ by using a parametrization of the pseudoscalar form factor $G_P(Q^2)$ motivated by the Goldberger-Treiman relation [44]. Two-body corrections are not included in this Letter. In our power-counting (see Ref. [43]), they are suppressed by at least one chiral order compared to their one-body counterparts.

To solve for the ground state of ^{16}O, we first solve the Hartree-Fock equations starting from the intrinsic Hamiltonian with two- and three-nucleon forces from chiral effective field theory. In a second step we normal-order the Hamiltonian with respect to the Hartree-Fock state keeping up to two-body terms, i.e., we use the normal-ordered two-body approximation [45,46]. Finally, we include beyond-mean-field correlations by employing the coupled-cluster (CC) method [38]. Notably, Eq. (2) includes a sum over the excited states of the nucleus, whose explicit calculation for ^{16}O is presently out of reach due to the many simultaneously open channels in the continuum. We circumvent the problem by using the Lorentz integral transform (LIT) method [47], which is based on integral transforming the response functions as

$$L_{\alpha\beta}(\sigma,\Gamma) = \frac{\Gamma}{\pi}\int d\omega \frac{R_{\alpha\beta}(\omega)}{(\omega-\sigma)^2+\Gamma^2} = \langle\tilde{\Psi}_\alpha|\tilde{\Psi}_\beta\rangle, \quad (7)$$

where Γ is the width and σ is the centroid of the Lorentzian kernel. In this approach, $|\tilde{\Psi}_{\alpha,\beta}\rangle$ are bound-state-like objects and are, therefore, easier to calculate than $|\Psi_f\rangle$. From a numerical inversion of the transform we eventually retrieve the response functions, which include the full final state interaction (FSI) [47]. The LIT method has been extensively used in few-body systems, also for electron [48] and neutrino scattering [49]. Here, we use it in conjunction with CC, adopting the so-called LIT-CC method, which has been previously applied to photo-absorption and electron-nucleus reactions [50–56].

Uncertainty quantification—The uncertainties in our *ab initio* calculations pertain to three main domains: (i) the truncation of the chiral effective field theory, (ii) the inversion of the LIT, and (iii) truncations in the many-body theory. Below, we explain how we assess them.

To estimate the uncertainty arising from the truncation of the chiral expansion of the nuclear potentials, we use the Gaussian Process (GP) error model [57]. We start from interactions at next-to leading $[\Delta\text{NLO}_{\text{GO}}(450)]$ and next-to-next-to leading order $[\Delta\text{NNLO}_{\text{GO}}(450)]$ explicitly including Δ-degrees of freedom [58]. We then fit a GP whose statistical properties provide estimates of the contribution of neglected terms that are higher order in p/Λ_χ. For further verification and for obtaining smooth $\mathcal{O}(1)$ curves to which the GP model can be fit, we compute observables also with the NNLO_{sat} potential [59] in the Δ-less chiral theory and use it as a reference to normalize the fit data. The GP model allows us to validate our choices of p and Λ_χ; see Refs. [60,61] for details. We explored different choices and found that $p \approx 250$ MeV and $\Lambda_\chi \approx 450$ MeV provide the best GP fits under the diagnostic criteria discussed in Ref. [57]. We therefore adopt these values in our uncertainty quantification. We notice that the former is roughly equal to the Fermi momentum of a nucleon in the nucleus and the latter corresponds to the cutoff of the chiral interactions used in this Letter. Regarding the chiral expansion of the electroweak current operator, we retain only one-body terms and neglect two-body contributions. In our power counting [62], two-body terms appear at higher order, and therefore their effect is expected to be smaller than the truncation error estimated from the potentials.

For the inversion of the LIT, we follow the strategy already used in Refs. [55,56], where we expand the response function in terms of a linear combination of N basis states that depend on a nonlinear parameter. We determine the N linear coefficients by a least-squares fit [47]. We estimate the uncertainty associated with the inversion procedure by performing several LIT inversions: we use two different values of $\Gamma = 5$, 10 MeV, vary N from 6 to 8, and use $n_0 = 0.5$, 1.5, a nonlinear parameter of the basis states which governs the threshold behavior [55].

To estimate the uncertainty in the many-body theory we proceed as follows. We calculate all observables in the coupled-cluster singles and doubles scheme (CCSD) [37,38] for an underlying harmonic oscillator frequency of $\hbar\Omega = 14$ MeV and a model space of 15 major oscillator shells ($N_{\max} = 2n + l = 14$). A cut for matrix elements of three-body forces $e_{3\,\max} = 2(n_1+n_2+n_3)+l_1+l_2+l_3 \leq 16$ has also been imposed. We checked that our results are well converged with respect to $N_{\max}$. In fact, varying $\hbar\Omega$ in the 14–20 MeV range contributes negligibly to the overall uncertainty. Effects from neglected triples excitations in the CC method are not included in the present analysis. Preliminary calculations including triples indicate that their effect is negligible in the quasielastic peak. A more thorough analysis is left for future work.

Overall, among the three uncertainties, (i) and (ii) dominate, while (iii) is negligible. All uncertainties are summed in quadrature and represented as bands in the figures. The chiral truncation uncertainty, (i), shown as a lighter band, dominates in the quasielastic peak and in the high-energy tail, while the LIT inversion uncertainty, (ii), depicted as a darker band, dominates near the threshold.

Results—In Fig. 1, we present our LIT-CC calculation of the $^{16}\text{O}(e,e')$ reaction at $E = 537$ MeV and $\theta = 37.1°$ (for momentum transfer $q \sim 330$ MeV/c) and compare it to calculations based on the spectral function (SF) formalism [63] and to data from Refs. [64,65]. Experimentally, the ^{12}C-α breakup threshold is located 7.162 MeV [66], slightly above the first 0^+ excited state. The 0^+ excited state is known to have a α-cluster structure [67] which is not well described at the CCSD approximation level. Therefore, the ^{12}C-α is not the first breakup channel in our calculations, but rather the proton-emission channel. To determine this threshold energy, we compute the proton separation energy using the particle-removed CC method truncated at the two-hole-one-particle excitation level [37,38,68],

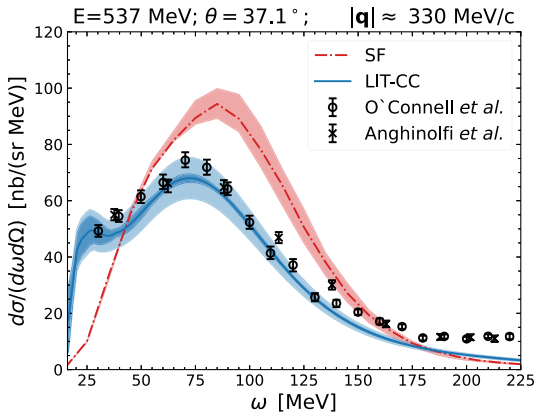

FIG. 1. $^{16}\text{O}(e,e')$ differential cross section as a function of the energy transfer: LIT-CC and SF calculations with corresponding uncertainties (see text for details) compared with experimental data from Refs. [64,65].

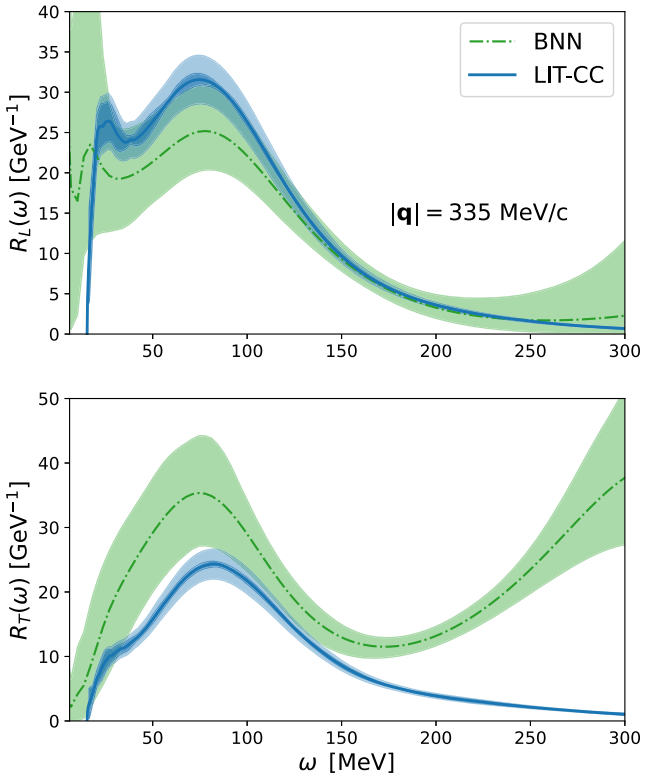

FIG. 2. ^{16}O longitudinal (upper panel) and transverse (lower panel) response functions: LIT-CC calculations with corresponding uncertainties (see text for details), compared with the neural network predictions from Ref. [69].

obtaining 10.6 MeV and 11.7 MeV for NNLOsat and $\Delta\text{NNLO}_{\text{GO}}(450)$, respectively, in fair agreement with the experimental value of 12.1 MeV [66]. We observe several bound excited states between 7 and 12 MeV with various multipolarities other than 0^+, which we remove before inverting, similar to what was done in Ref. [55]. Finally, to compare with the data taken at a fixed electron-scattering angle, we performed several calculations on a grid of momentum transfers, using a mesh spacing of 10 MeV, and interpolated linearly between the points.

In Fig. 1, we see that the full treatment of the FSI achieved by the LIT-CC results gives an excellent description of data. While the SF approach, where the plane-wave impulse approximation is used, overestimates the data in the quasielastic peak, as expected in this momentum regime. The uncertainty of the SF result comes from the propagation of the error in the spectral reconstruction of the SF computed within the coupled-cluster method. Typically, the SF approach works well for $q > 500$ MeV/c [63].

The measurements in Refs. [64,65] did not perform a Rosenbluth separation; therefore, we cannot individually compare the calculated electromagnetic response functions R_L and R_T with experimental data. However, we can compare them with the prediction obtained from the Bayesian neutral network (BNN) devised in Ref. [69] which is trained on the (e, e') scattering data of several symmetric

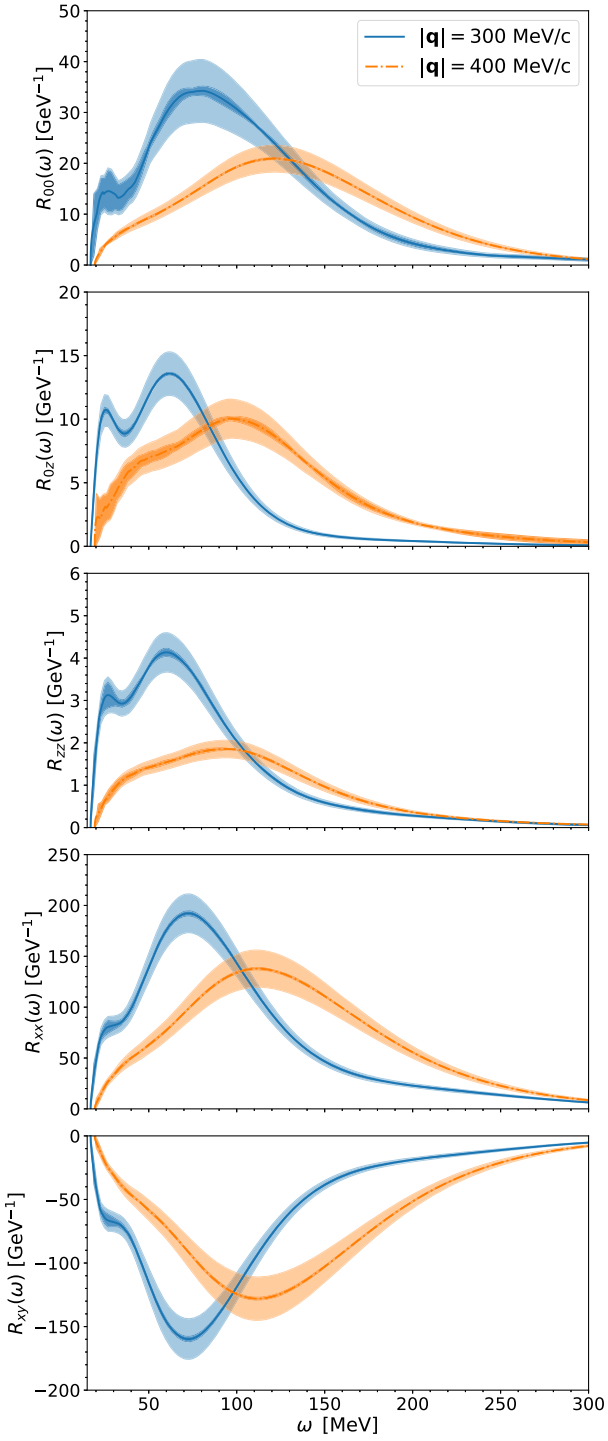

FIG. 3. Five different charge-current response functions related to the $^{16}\text{O}(\nu_l, l^-)$ reaction for $q = 300$, 400 MeV/c with corresponding uncertainties (see text for details).

nuclei. Such a comparison is presented in Fig. 2 for the momentum transfer value $q = 335$ MeV/c and energy transfer from 0 to 300 MeV. The BNN predictions are shown with the corresponding uncertainty, which is quite large in this case due to the scarsity of available data for ^{16}O.

We observe that the BNN and LIT-CC results are compatible, particularly at low energy, while a discrepancy is seen for R_T beyond the quasielastic peak, where the BNN prediction is consistently larger. This discrepancy can be understood in light of the fact that the LIT-CC calculation only includes one-body currents and does not account for pion production mechanisms. The neglected two-body currents would typically enhance the quasielastic peak [28], as would the Δ-isobar currents, which are expected to cause the rise in the response beyond $\omega = 200$ MeV predicted by the BNN. We note that the ≈15–20% deficit in R_T strength in the quasielastic peak region cannot be easily appreciated in Fig. 1, as the cross section is dominated by the longitudinal response at this kinematic setup.

We now turn to the discussion of the five ^{16}O weak response functions: $R_{00}, R_{zz}, R_{0z}, R_{xx}$, and R_{xy}. These functions are computed for two momentum transfers, $q = 300$ MeV/c and $q = 400$ MeV/c, using 8 and 11 multipoles, respectively, to achieve convergence in the decomposition of the electroweak current operator. When inverting the LIT, we impose the threshold energy of the $^{16}\mathrm{O}(\nu_e, e)\mathrm{p}^{15}\mathrm{O}$ channel amounting to 12.5 MeV and 13.6 MeV for $\mathrm{NNLO_{sat}}$ and $\Delta\mathrm{NNLO_{GO}}(450)$, respectively, which compares relatively well with the experimental value of 14.4 MeV. As in the electromagnetic case, several excited states below the nucleon-emission threshold were identified and removed.

In Fig. 3, similar to the electromagnetic case, the weak response functions exhibit a shoulder structure near the threshold. This feature was also observed in our LIT-CC calculations for ^{4}He [55] but not in the Quantum Monte Carlo calculations for ^{12}C [30]. The difference may stem from variations in the employed Hamiltonian, the many-body method, or the nucleus itself. The position of the quasielastic peak in the weak response functions is approximately the same as in the electromagnetic case. As expected, and consistent with other findings [30], the peak shifts to higher energies and its strength diminishes as the momentum transfer increases. Finally, the uncertainties in the results for $q = 300$ and $q = 400$ MeV/c are generally comparable in size, except for the R_{00} response, where a larger uncertainty at $q = 300$ MeV/c is observed due to larger differences between the predictions of different chiral potentials.

Conclusions—Quasielastic lepton-nucleus scattering plays a crucial role in experimental programs aimed at studying fundamental neutrino properties, necessitating thorough calculations. Here, we compute and quantify the uncertainties associated with a set of properties related to $^{16}\mathrm{O}(e, e')$ and $^{16}\mathrm{O}(\nu_l, l^-)$ scattering in the *ab initio* LIT-CC framework using chiral forces. The observed agreement with available electron-scattering data and BNN-reconstructed responses provides an important validation of our approach. Additionally, computations of electroweak responses are a key input for future analyses of neutrino scattering on oxygen targets. For low-momentum transfers, where the plane-wave impulse approximation is not valid, these computationally intensive results could serve as a direct link to the analysis of experimental data if integrated into Monte Carlo event generators.

This Letter represents the first attempt to provide *ab initio* computations of electroweak reactions in the mass range of $A = 16$ with quantified uncertainties. We estimate uncertainties from different sources: some originate from the many-body method and numerical procedures, which are dominant at low-energy transfer, while others stem from the truncation of the effective field theory used to model the strong force, which dominate at higher energies and are evaluated using modern statistical tools. Overall, our uncertainty estimates are reasonable and comparable to experimental errors when available. The potential to improve and reduce theoretical uncertainties makes our approach very promising. Future work in this area will involve studying higher-order many-body correlations and the effects of two-body currents.

Acknowledgments—We acknowledge useful discussions with Thomas Papenbrock. This work was supported by the Deutsche Forschungsgemeinschaft (DFG) through the Cluster of Excellence "Precision Physics, Fundamental Interactions, and Structure of Matter" (PRISMA$^+$ EXC 2118/1, Project ID No. 390831469) and through the Collaborative Research Center "Hadron and Nuclei as discovery tools" (Project ID No. 514321794); the European Union's Horizon 2020 research and innovation programme under the Marie Skłodowska-Curie Grant Agreement No. 101026014; the Office of Nuclear Physics, U.S. Department of Energy under Contract No. DE-AC05-00OR22725 with Oak Ridge National Laboratory and under SciDAC-5 (NUCLEI Collaboration); and the Office of High Energy Physics, U.S. Department of Energy under Contract No. DE-AC02-07CH11359 through the Neutrino Theory Network Fellowship Program. Computer time was provided by the Innovative and Novel Computational Impact on Theory and Experiment (INCITE) program. This research used resources from the Oak Ridge Leadership Computing Facility located at ORNL, which is supported by the Office of Science of the Department of Energy under Contract No. DE-AC05-00OR22725, as well as the supercomputer MogonII at Johannes Gutenberg-Universität Mainz.

This manuscript has been authored by UT-Battelle, LLC, under Contract No. DE-AC05-00OR22725 with the U.S. Department of Energy (DOE). The U.S. government retains and the publisher, by accepting the article for publication, acknowledges that the U.S. government retains a nonexclusive, paid-up, irrevocable, worldwide license to publish or reproduce the published form of this manuscript, or

allow others to do so, for U.S. government purposes. DOE will provide public access to these results of federally sponsored research in accordance with the DOE Public Access Plan [70].

[1] Alexander L. Fetter and John Dirk Walecka, *Quantum Theory of Many-Particle Systems* (McGraw-Hill, New York, 1971).

[2] Peter Ring and Peter Schuck, *The Nuclear Many-Body Problem* (Springer, Berlin, Heidelberg, 2004).

[3] Willem H. Dickhoff and Dimitri Van Neck, *Many-Body Theory Exposed!* (World Scientific, Singapore, 2005).

[4] Winfried Leidemann and Giuseppina Orlandini, Modern *ab initio* approaches and applications in few-nucleon physics with A $\geq$ 4, Prog. Part. Nucl. Phys. **68**, 158 (2013).

[5] Sonia Bacca and Saori Pastore, Electromagnetic reactions on light nuclei, J. Phys. G **41**, 123002 (2014).

[6] Evgeny Epelbaum, Hans-Werner Hammer, and Ulf-G. Meissner, Modern theory of nuclear forces, Rev. Mod. Phys. **81**, 1773 (2009).

[7] R. Machleidt and D. R. Entem, Chiral effective field theory and nuclear forces, Phys. Rep. **503**, 1 (2011).

[8] H.-W. Hammer, Sebastian König, and U. van Kolck, Nuclear effective field theory: Status and perspectives, Rev. Mod. Phys. **92**, 025004 (2020).

[9] H. Hergert, A guided tour of *ab initio* nuclear many-body theory, Front. Phys. **8**, 379 (2020).

[10] A. Ekström, C. Forssén, G. Hagen, G. R. Jansen, W. Jiang, and T. Papenbrock, What is *ab initio* in nuclear theory?, Front. Phys. **11**, 1129094 (2023).

[11] Babak Abi *et al.* (DUNE Collaboration), Deep underground neutrino experiment (DUNE), far detector technical design report, volume II: DUNE physics, arXiv:2002.03005.

[12] R. Acciarri *et al.* (DUNE Collaboration), Long-baseline neutrino facility (LBNF) and deep underground neutrino experiment (DUNE), arXiv:1512.06148.

[13] K. Abe *et al.* (Hyper-Kamiokande Proto-Collaboration), Physics potential of a long-baseline neutrino oscillation experiment using a J-PARC neutrino beam and Hyper-Kamiokande, Prog. Theor. Exp. Phys. **2015**, 053C02 (2015).

[14] L. Alvarez Ruso *et al.*, Theoretical tools for neutrino scattering: Interplay between lattice QCD, EFTs, nuclear physics, phenomenology, and neutrino event generators, J. Phys. G **52**, 043001 (2025).

[15] https://discovery.phys.virginia.edu/research/groups/qes-archive/

[16] W. C. Haxton, Nuclear response of water Cherenkov detectors to supernova and solar neutrinos, Phys. Rev. D **36**, 2283 (1987).

[17] R. C. Allen, H. H. Chen, P. J. Doe, R. Hausamann, W. P. Lee, X.-Q. Lu, H. J. Mahler, M. E. Potter, K. C. Wang, T. J. Bowles, R. L. Burman, R. D. Carlini, D. R. F. Cochran, J. S. Frank, E. Piasetzky, V. D. Sandberg, D. A. Krakauer, and R. L. Talaga, Measurement of the exclusive cross section ^{12}C$(\nu_e, e^-)^{12}$n(g.s.), Phys. Rev. Lett. **64**, 1871 (1990).

[18] B Zeitnitz, Karmen: Neutrino physics at ISIS, Prog. Part. Nucl. Phys. **32**, 351 (1994).

[19] O. Benhar, A. Fabrocini, S. Fantoni, and I. Sick, Spectral function of finite nuclei and scattering of GeV electrons, Nucl. Phys. **A579**, 493 (1994).

[20] E. Kolbe, K. Langanke, F.-K. Thielemann, and P. Vogel, Inclusive ^{12}C$(\nu_\mu, \mu)^{12}$n reaction in the continuum random phase approximation, Phys. Rev. C **52**, 3437 (1995).

[21] N. Auerbach, N. Van Giai, and O. K. Vorov, Neutrino scattering from ^{12}C and ^{16}O, Phys. Rev. C **56**, R2368 (1997).

[22] L. B. Auerbach *et al.* (LSND Collaboration), Measurements of charged current reactions of muon neutrinos on ^{12}C, Phys. Rev. C **66**, 015501 (2002).

[23] A. C. Hayes and I. S. Towner, Shell-model calculations of neutrino scattering from ^{12}C, Phys. Rev. C **61**, 044603 (2000).

[24] H. Dai *et al.* (Jefferson Lab Hall A Collaboration), First measurement of the Ar$(e, e')X$ cross section at Jefferson Laboratory, Phys. Rev. C **99**, 054608 (2019).

[25] C. Barbieri, N. Rocco, and V. Somà, Lepton scattering from ^{40}Ar and Ti in the quasielastic peak region, Phys. Rev. C **100**, 062501(R) (2019).

[26] Artur M. Ankowski and Alexander Friedland, Assessing the accuracy of the GENIE event generator with electron-scattering data, Phys. Rev. D **102**, 053001 (2020).

[27] M. Mihovilovič *et al.*, Measurement of the ^{12}C(e, e') cross sections at $Q^2 = 0.8\ \mathrm{GeV}^2/c^2$, Few-Body Syst. **65**, 78 (2024).

[28] A. Lovato, S. Gandolfi, J. Carlson, Steven C. Pieper, and R. Schiavilla, Electromagnetic response of ^{12}C: A first-principles calculation, Phys. Rev. Lett. **117**, 082501 (2016).

[29] A. Lovato, S. Gandolfi, J. Carlson, Ewing Lusk, Steven C. Pieper, and R. Schiavilla, Quantum Monte Carlo calculation of neutral-current $\nu - ^{12}C$ inclusive quasielastic scattering, Phys. Rev. C **97**, 022502(R) (2018).

[30] A. Lovato, J. Carlson, S. Gandolfi, N. Rocco, and R. Schiavilla, *Ab initio* study of (ν_ℓ, ℓ^-) and $(\bar{\nu}_\ell, \ell^+)$ inclusive scattering in ^{12}C: Confronting the MiniBooNE and T2K CCQE data, Phys. Rev. X **10**, 031068 (2020).

[31] Evgeny Epelbaum, Hermann Krebs, Timo A. Lähde, Dean Lee, and Ulf-G. Meißner, Structure and rotations of the Hoyle state, Phys. Rev. Lett. **109**, 252501 (2012).

[32] T. Otsuka, T. Abe, T. Yoshida, Y. Tsunoda, N. Shimizu, N. Itagaki, Y. Utsuno, J. Vary, P. Maris, and H. Ueno, α-clustering in atomic nuclei from first principles with statistical learning and the Hoyle state character, Nat. Commun. **13**, 2234 (2022).

[33] C. G. Payne, S. Bacca, G. Hagen, W. Jiang, and T. Papenbrock, Coherent elastic neutrino-nucleus scattering on ^{40}Ar from first principles, Phys. Rev. C **100**, 061304(R) (2019).

[34] F. Coester, Bound states of a many-particle system, Nucl. Phys. **7**, 421 (1958).

[35] F. Coester and H. Kümmel, Short-range correlations in nuclear wave functions, Nucl. Phys. **17**, 477 (1960).

[36] D. J. Dean and M. Hjorth-Jensen, Coupled-cluster approach to nuclear physics, Phys. Rev. C **69**, 054320 (2004).

[37] Rodney J. Bartlett and Monika Musiał, Coupled-cluster theory in quantum chemistry, Rev. Mod. Phys. **79**, 291 (2007).

[38] G. Hagen, T. Papenbrock, M. Hjorth-Jensen, and D. J. Dean, Coupled-cluster computations of atomic nuclei, Rep. Prog. Phys. **77**, 096302 (2014).

[39] T. Miyagi, S. R. Stroberg, J. D. Holt, and N. Shimizu, *Ab initio* multishell valence-space Hamiltonians and the island of inversion, Phys. Rev. C **102**, 034320 (2020).

[40] J. M. Yao, B. Bally, J. Engel, R. Wirth, T. R. Rodríguez, and H. Hergert, *Ab initio* treatment of collective correlations and the neutrinoless double beta decay of ^{48}Ca, Phys. Rev. Lett. **124**, 232501 (2020).

[41] Mikael Frosini, Thomas Duguet, Jean-Paul Ebran, Benjamin Bally, Tobias Mongelli, Tomás R. Rodríguez, Robert Roth, and Vittorio Somà, Multi-reference many-body perturbation theory for nuclei: II. *Ab initio* study of neon isotopes via PGCM and IM-NCSM calculations, Eur. Phys. J. A **58**, 63 (2022).

[42] Z. H. Sun, A. Ekström, C. Forssén, G. Hagen, G. R. Jansen, and T. Papenbrock, Multiscale physics of atomic nuclei from first principles, Phys. Rev. X **15**, 011028 (2025).

[43] Bijaya Acharya and Sonia Bacca, Neutrino-deuteron scattering: Uncertainty quantification and new $L_{1,A}$ constraints, Phys. Rev. C **101**, 015505 (2020).

[44] Torleif Erik Oskar Ericson and W. Weise, *Pions and Nuclei* (Clarendon Press, Oxford, United Kingdom, 1988).

[45] G. Hagen, T. Papenbrock, D. J. Dean, A. Schwenk, A. Nogga, M. Włoch, and P. Piecuch, Coupled-cluster theory for three-body Hamiltonians, Phys. Rev. C **76**, 034302 (2007).

[46] Robert Roth, Sven Binder, Klaus Vobig, Angelo Calci, Joachim Langhammer, and Petr Navrátil, Medium-mass nuclei with normal-ordered chiral $NN+3N$ interactions, Phys. Rev. Lett. **109**, 052501 (2012).

[47] V. D. Efros, W. Leidemann, G. Orlandini, and N. Barnea, The Lorentz Integral Transform (LIT) method and its applications to perturbation-induced reactions, J. Phys. G **34**, R459 (2007).

[48] S. Bacca, H. Arenhoevel, N. Barnea, W. Leidemann, and G. Orlandini, Inclusive electron scattering off ^{4}He, Phys. Rev. C **76**, 014003 (2007).

[49] Doron Gazit and Nir Barnea, Low-energy inelastic neutrino reactions on ^{4}He, Phys. Rev. Lett. **98**, 192501 (2007).

[50] S. Bacca, N. Barnea, G. Hagen, G. Orlandini, and T. Papenbrock, First principles description of the giant dipole resonance in ^{16}**O**, Phys. Rev. Lett. **111**, 122502 (2013).

[51] S. Bacca, N. Barnea, G. Hagen, M. Miorelli, G. Orlandini, and T. Papenbrock, Giant and pigmy dipole resonances in ^{4}He, ^{16,22}O, and ^{40}Ca from chiral nucleon-nucleon interactions, Phys. Rev. C **90**, 064619 (2014).

[52] M. Miorelli, S. Bacca, N. Barnea, G. Hagen, G. R. Jansen, G. Orlandini, and T. Papenbrock, Electric dipole polarizability from first principles calculations, Phys. Rev. C **94**, 034317 (2016).

[53] M. Miorelli, S. Bacca, G. Hagen, and T. Papenbrock, Computing the dipole polarizability of ^{48}Ca with increased precision, Phys. Rev. C **98**, 014324 (2018).

[54] J. Simonis, S. Bacca, and G. Hagen, First principles electromagnetic responses in medium-mass nuclei—Recent progress from coupled-cluster theory, Eur. Phys. J. A **55**, 241 (2019).

[55] J. E. Sobczyk, B. Acharya, S. Bacca, and G. Hagen, *Ab initio* computation of the longitudinal response function in ^{40}Ca, Phys. Rev. Lett. **127**, 072501 (2021).

[56] J. E. Sobczyk, B. Acharya, S. Bacca, and G. Hagen, ^{40}Ca transverse response function from coupled-cluster theory, Phys. Rev. C **109**, 025502 (2024).

[57] J. A. Melendez, R. J. Furnstahl, D. R. Phillips, M. T. Pratola, and S. Wesolowski, Quantifying correlated truncation errors in effective field theory, Phys. Rev. C **100**, 044001 (2019).

[58] W. G. Jiang, A. Ekström, C. Forssén, G. Hagen, G. R. Jansen, and T. Papenbrock, Accurate bulk properties of nuclei from $a = 2$ to ∞ from potentials with Δ isobars, Phys. Rev. C **102**, 054301 (2020).

[59] A. Ekström, G. R. Jansen, K. A. Wendt, G. Hagen, T. Papenbrock, B. D. Carlsson, C. Forssén, M. Hjorth-Jensen, P. Navrátil, and W. Nazarewicz, Accurate nuclear radii and binding energies from a chiral interaction, Phys. Rev. C **91**, 051301(R) (2015).

[60] Bijaya Acharya and Sonia Bacca, Gaussian process error modeling for chiral effective-field-theory calculations of np $\leftrightarrow$ dγ at low energies, Phys. Lett. B **827**, 137011 (2022).

[61] Bijaya Acharya, Uncertainty estimation and anomaly detection in chiral effective field theory studies of key nuclear electroweak processes, Few-Body Syst. **65**, 65 (2024).

[62] Daniel R. Phillips, Electromagnetic structure of two- and three-nucleon systems: An effective field theory description, Annu. Rev. Nucl. Part. Sci. **66**, 421 (2016).

[63] Joanna E. Sobczyk and Sonia Bacca, ^{16}O spectral function from coupled-cluster theory: Applications to lepton-nucleus scattering, Phys. Rev. C **109**, 044314 (2024).

[64] J. S. O'Connell *et al.*, Electromagnetic excitation of the delta resonance in nuclei, Phys. Rev. C **35**, 1063 (1987).

[65] M. Anghinolfi *et al.*, Quasi-elastic and inelastic inclusive electron scattering from an oxygen jet target, Nucl. Phys. **A602**, 405 (1996).

[66] M. Wang, G. Audi, A. H. Wapstra, F. G. Kondev, M. MacCormick, X. Xu, and B. Pfeiffer, The Ame2012 atomic mass evaluation, Chin. Phys. C **36**, 1603 (2012).

[67] Evgeny Epelbaum, Hermann Krebs, Timo A. Lähde, Dean Lee, Ulf-G. Meißner, and Gautam Rupak, *Ab initio* calculation of the spectrum and structure of ^{16}O, Phys. Rev. Lett. **112**, 102501 (2014).

[68] J. R. Gour, P. Piecuch, M. Hjorth-Jensen, M. Włoch, and D. J. Dean, Coupled-cluster calculations for valence systems around ^{16}O, Phys. Rev. C **74**, 024310 (2006).

[69] Joanna E. Sobczyk, Noemi Rocco, and Alessandro Lovato, Modeling inclusive electron-nucleus scattering with Bayesian artificial neural networks, Phys. Lett. B **859**, 139142 (2024).

[70] https://www.energy.gov/doe-public-access-plan